

Repository Istituzionale dei Prodotti della Ricerca del Politecnico di Bari

Morphological optimization of tensegrity-type metamaterials

This is a pre-print of the following article

Original Citation:
Morphological optimization of tensegrity-type metamaterials / De Tommasi, D., Marano, G.C., Puglisi, G., Trentadue, F.. - In: COMPOSITES. PART B, ENGINEERING. - ISSN 1359-8368. - STAMPA. - 115:(2017), pp. 182-187. [10.1016/j.compositesb.2016.10.017]

Availability:
This version is available at http://hdl.handle.net/11589/131548 since: 2021-03-06

Published version
DOI:10.1016/j.compositesb.2016.10.017

Publisher:

Terms of use:

(Article begins on next page)

17 November 2026

*Detailed Response to Reviewers

Revisions to Morphological optimization of tensegrity-type metamaterials

D. De Tommasi, G.C. Marano, G. Puglisi, F. Trentadue.

Dip. Scienze Ingegneria Civile e Architettura, Politecnico di Bari, Via Re David 200, Bari, Italy

---

Reviewer 1: References incomplete. Authors of Composites B should cite relevant papers, especially from same journal. Some of the concepts are quite advanced or too lengthy to describe them, thus, references must be as complete as possible. The English should be improved as well; I would recommend double checking the text before re-submission.

We added references 11 and 12
We ask to a native speaker and corrected the English language
We added Fig. 2 with a comment on it.

*Manuscript
Click here to view linked References

Morphological optimization of tensegrity-type metamaterials

D. De Tommasi, G.C. Marano, G. Puglisi, F. Trentadue.

Dip. Scienze Ingegneria Civile e Architettura, Politecnico di Bari, Via Re David 200, Bari, Italy

Abstract

We analyze the problem of morphological optimization for metamaterials with tensegrity-type cells. Our mass and morphological optimization scheme is based on both local and global instability analyses. As a meaningful prototypical example we tassellate a slab, subjected to a compression macro-stress orthogonal to its middle plane, into periodic patterns of triangular, square and hexagonal cells.

Keywords: Metamaterials, Morphological Optimization, Tensegrities, Global Stability

1. Introduction

Metamaterials are engineered materials, which may exhibit resistance and lightness properties unobserved in natural materials [2], [3]. Strong and lightweight materials are increasingly needed for several advanced applications as those in aerospace and automotive fields. The new proposed materials are typically obtained as periodically patterned low scale structures, whose macroscopic response depends primarily on their topology rather than chemical composition. Thus understanding how the topology of the structured material influences the macroscopic properties is a key-point to propose design criteria for new artificial materials. The interest in this field is also due to other physical properties of the new designed materials, such as optical properties [4], negative material moduli [7] and vanishing macroscopic shear modulus [8].

The present study is based on previous results on the mass optimality of tensegrity structures for compressive load transfer [9], [10]. Here we ana-

lyze the morphological optimization of metamaterials based on the tensegrity concept [5], [1], [11], [12]. In particular, we consider a prototypical model of an infinite slab undergoing a uniform compressive macro-stress. With the aim of enhancing the structure lightness, we *design* a periodic array of identical tensegrity *cells* supporting the same compressive load. Based on a well known result on planar tessellation, we consider three different periodic patterns of cells, whose sections on the middle plane of the slab are equilateral triangles, squares and regular hexagons (see Fig 1).

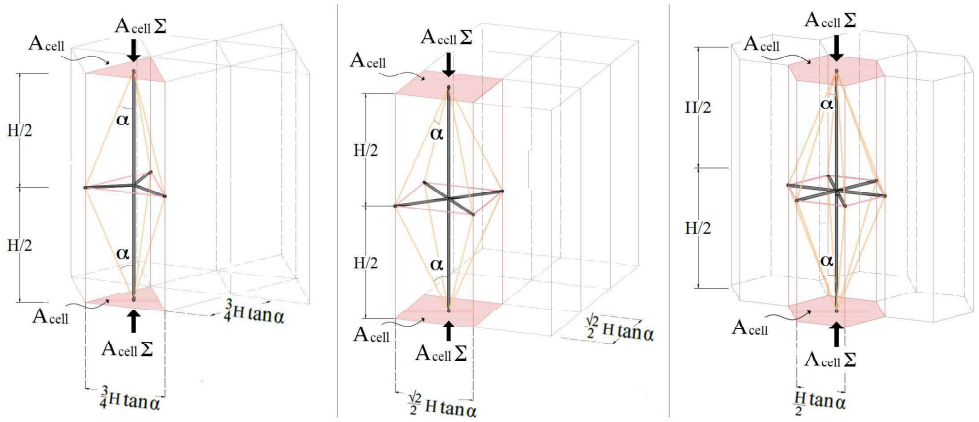


Figure 1: Scheme of the three tensegrity-type metamaterials (equilateral triangles, squares, regular hexagons)

As already observed in other works (see e.g. [6], [9]), the main drawback of the light designed metamaterials is the onset of both local and global instability effects, both due to slender struts and to the multiplicity of equilibrium solutions due to the strong geometrical nonlinearity of the problem. Thus, our optimization scheme aims to obtain the geometrical and prestress variables realizing the minimum mass value and relies on the assumption that each cell satisfies both local and global stability conditions, together with material resistance. In particular, a local otimization procedure is adopted for the present analysis. Finally, the morphological optimization is achieved by comparing the optimum volume of the three tensegrity classes, showing that the *hexagonal cell corresponds to the minimum mass metamaterial.*

An important possible improvement of our solution is to consider for each class of metamaterials the possibility of a hierarchical refinement, substitut-

ing struts with self similar tensegrities. Indeed in [9, 10] the authors showed the possibility of strongly decreasing a tensegrity weight by increasing its complexity.

2. Morphological optimization

As already exposed, our scheme for material optimization is based on a partition of a slab into a periodic sequence of tensegrity cells with three different shapes (see the schemes in Fig.1). In particular we consider three different, symmetric, tensegrity cells having cross sections in the middle plane of the slab with triangular, square and hexagonal shapes. Our choice is based on the classical geometrical result by which the only tessellation of the plane into identical regular polygons is given by equilateral triangles, squares or regular hexagons.

We assume that a normal compression macro-stress Σ is applied on the external plane surfaces, so that the load applied to the single tensegrity cell (see Fig. 1) is

$$P = A_{cell}\Sigma. \tag{1}$$

Here the tranversal area is given by

$$A_{cell} = \frac{p\,H^2}{8}\cos\left(\frac{2\pi}{p}\right)\tan^2\alpha, \qquad p = 3, 4, 6, \tag{2}$$

where p is the number of sides of the polygonal cross section. We introduce the following assumptions:

i) cables undergo only traction forces both in the loaded and unloaded states and the internal forces respect the condition of material failure;

ii) struts undergo only compression axial forces and, both in the loaded and unloaded states, the conditions of material failure and local Euler buckling are satisfied;

iii) the loaded configuration is *globally stable.*

Under the above assumptions, we aim to minimize the volume density

$$\rho := \frac{\textit{tensegrity volume}}{A_{cell}H},$$

where *tensegrity volume* is the global volume of all members of a tensegrity cell and A_{cell} is given by (2).

A similar problem, in a two-dimensional setting, was proposed in [9, 10] where explicit solutions have been obtained. We thus refer the reader to these works for a detailed analytical discussion of the problem, while we here extend to the three-dimensional case the problem in a numerical setting.

2.1. Elastic equilibrium of tensegrity cells

The optimal metamaterial is designed considering both the loaded and the unloaded state. The unloaded (prestressed) configuration is assumed as reference configuration, while the loaded configuration presents a homogeneous contraction in the direction orthogonal to the middle plane and a homogeneous extension in the middle plane of the slab.

Consider now a tensegrity cell, that in the terminology of [13] is assigned by a T-bar (see Fig.1) characterized by the same height H of the slab. Due to the periodicity and the symmetry properties of the metamaterial, any tensegrity cell is two-degrees statically indeterminate. To describe the internal forces in the *loaded state* ($P = \Sigma A_{cell}$) we consider the two parameters β and τ, defined as follows:

$$\begin{cases} \beta &= \frac{N}{P} > 1 \\ \tau &= \frac{T_{ct}}{P} > 0 \end{cases}, \tag{3}$$

where N is the compression force in the principal struts and T_{ct} is the traction force in the transverse cables on the middle plane. By imposing the equilibrium in the loaded state we find the following axial internal forces:

$$\begin{cases} N &= \beta P \\ N_t &= \dfrac{2}{p}(\beta - 1)P \tan\alpha + 2\tau \sin\dfrac{\pi}{p} \\ T &= \dfrac{(\beta - 1)P}{p\cos\alpha} \\ T_t &= \tau P \end{cases}, \tag{4}$$

where: α is the angle formed by the principal struts and the principal cables (see Fig. 1); T and N_t are the traction force in the principal cables and the compression force in the transversal struts, respectively. In the unloaded state ($P = 0$) we choose to describe the prestress by the parameter $\overline{\beta}$ and $\overline{\tau}$, having analogous meaning of β and τ. By using superposition, we determine the following relation between the two parameters in the loaded and unloaded

states

$$\begin{cases} \bar{\beta} &= \beta + \tilde{N}_{[1]} \\ \bar{\tau} &= \tau + \tilde{T}_{ct[1]} \end{cases} . \tag{5}$$

Here $\tilde{N}_{[1]}$ is the (negative) compression force induced in the principal strut by a unitary traction force ($P = -1$) and $\tilde{T}_{ct[1]}$ is the (negative) traction force induced in the tranversal cables by the same external force. The explicit expression of these quantities is not given here for sake of brevity.

Finally, the equilibrium conditions give the following relations for the axial forces in the unload state:

$$\begin{cases} \bar{N} &= \bar{\beta} P \\ \bar{N}_t &= \dfrac{2}{p} \bar{\beta} P \tan\alpha + 2\bar{\tau} \sin\dfrac{\pi}{p} \\ \bar{T} &= \dfrac{\bar{\beta} P}{p \cos\alpha} \\ \bar{T}_t &= \bar{\tau} P \end{cases} . \tag{6}$$

2.2. Global stability analysis

In the stability analysis we do not consider localization effects, that is we assume that all cells undergo the same critical displacements. Consider a T-Bar of length H, subjected to an axial force P. We suppose that the material is homogeneous with Young modulus E. We measure the incremental displacements from the homogeneously deformed loaded configuration. Pre-critical displacements are assumed small and then the deformed lengths of the members are identified with the natural ones. The total potential energy (set equal to zero in the loaded state) can be written as

$$V(\boldsymbol{u}, P) = \sum_{k=1}^{2+3p} \left[N^{(k)} \Delta l^{(k)} + \frac{E A^{(k)}}{2} \left(\frac{\Delta l^{(k)}}{l^{(k)}} \right)^2 l^{(k)} \right] - 2 P u_1, \tag{7}$$

where

$$\Delta l^{(k)} = ||\Delta \boldsymbol{x}^{(k)} + \boldsymbol{T}^{(k)} \boldsymbol{u}|| - l^{(k)}.$$

Here: $\boldsymbol{u}$ is the vector of generalized incremental displacements; $2u_1$ is the contraction in the direction orthogonal to the middle plane of the slab; $l^{(k)}$ is the length of the (k)-th member, whose area and elongation are denoted by $A^{(k)}$ and $\Delta l^{(k)}$; $\Delta \boldsymbol{x}^{(k)}$ and $\boldsymbol{T}^{(k)} \boldsymbol{u}$ are the axial vector and the relative incremental displacement vector between the end joints of the (k)-th bar. In

particular, we have:

$$A^{(k)} = \begin{cases} A & k{=}1{,}2 \\ A_t & k{=}3{,}4{,}..{,}2{+}p \\ A_c & k{=}3{+}p{,}4{+}p{,}...{,}2{+}2p \\ A_{ct} & k{=}3{+}2p{,}4{+}2p{,}...{,}2{+}3p \end{cases} , \tag{8}$$

that is A and A_t are the areas of the cross sections of the principal and transversal struts respectively. Similarly we indicate by A_c and A_{ct} the cross section areas of the principal and traversal cables.

The lengths $l^{(k)}$ of the members are given by

$$l^{(k)} = \begin{cases} \frac{H}{2} & k{=}1{,}2 \\ \frac{H \tan\alpha}{2} & k{=}3{,}4{,}..{,}2{+}p \\ \frac{H}{2\cos\alpha} & k{=}3{+}p{,}4{+}p{,}...{,}2{+}2p \\ H \sin\frac{\pi}{p} \tan\alpha & k{=}3{+}2p{,}4{+}2p{,}...{,}2{+}3p \end{cases} . \tag{9}$$

The axial forces $N^{(k)}$ (numbered such as the lengths and the member areas) are given by (4). The tangent stiffness matrix $\boldsymbol{K}$ is the 9x9 Hessian matrix of the total potential energy in the loaded configuration:

$$\boldsymbol{K} = \frac{\partial^2 V}{\partial \boldsymbol{u} \partial \boldsymbol{u}} \bigg|_{\boldsymbol{u}=\boldsymbol{0}} . \tag{10}$$

The matrix $\boldsymbol{K}$ is imposed to be semidefinite positive:

$$\boldsymbol{K} \succeq \boldsymbol{0}. \tag{11}$$

The above positivity condition is imposed by requiring that its leading principal minors are all non-negative.

Based on the symmetry properties of the tensegrity cell, in our numerical analysis we choose symmetric and antisymmetric generalized displacements as shown in Fig.2 in the case of square cell. Thanks to this approach, the Hessian matrix $\boldsymbol{K}$ is a block diagonal matrix, with maximum 2x2 submatrices dimension. This is very important in the optimization procedure, since it significantly simplifies the numerical analysis of positiveness.

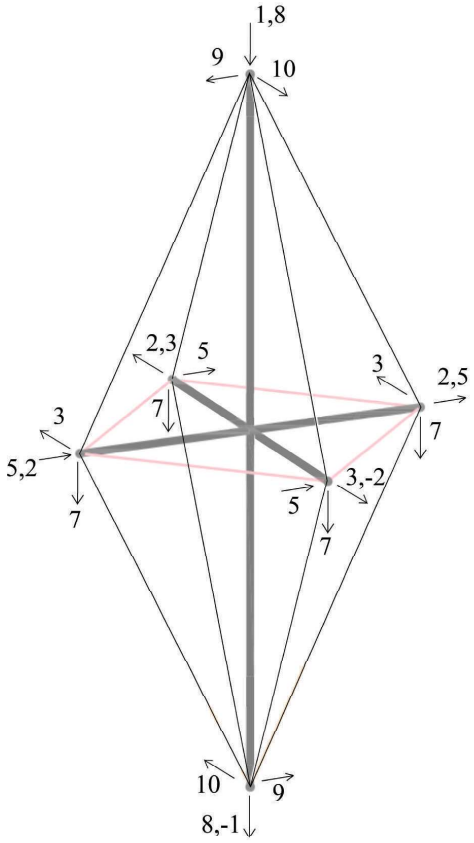


Figure 2: Scheme of the generalized displacements.

2.3. Constrained minimum problem

We choose the following design vector

$$\begin{aligned} \mathbf{x} &= \left\{ x_1 \quad x_2 \quad x_3 \quad x_4 \quad x_5 \quad x_6 \quad x_7 \right\}^T \\ &= \left\{ \frac{A\sigma_y}{P} \quad \frac{A_t\sigma_y}{P} \quad \frac{A_s\sigma_y}{P} \quad \frac{A_{sc}\sigma_y}{P} \quad \beta \quad \tau \quad \tan\alpha \right\}^T , \end{aligned} \tag{12}$$

where σ_y is the yield stress of the material, assumed unique for both struts and cables.

As already stated, we aim to minimize the volume density. Given the

design variables (12), this can be written as

$$\begin{aligned}\rho(\mathbf{x}) &= \frac{8\left(A+\frac{p}{2}A_t\tan\alpha+2p\,A_c\sqrt{1+\tan^2\alpha}+p\,A_{ct}\tan\alpha\,\sin\frac{\pi}{p}\right)}{p\cos\left(\frac{2\pi}{p}\right)H^2\tan^2\alpha}\\ &= \frac{8P\left(x_1+\frac{p}{2}x_2\,x_7+2p\,x_3\sqrt{1+x_7^2}+p\,x_4\,x_7\,\sin\frac{\pi}{p}\right)}{\sigma_y p\cos\left(\frac{2\pi}{p}\right)H^2x_7^2}\,.\end{aligned} \tag{13}$$

We suppose that all the bars have the same cross section shape and we indicate by $J=\frac{A^2}{\xi^2\pi^2}$ their axial area moment (here ξ depends only on the form of the cross section). In view of the assumptions (i)-(iii) and of the equations (4)-(5), the design variables must satisfy a set of inequalities defining the feasible set $\mathcal{X}$

$$\mathcal{X}\ni\mathbf{x} \iff \begin{cases} x_1 \geq \max\left\{\frac{N}{P};\left(\xi\frac{l}{2}\sqrt{N/E}\right)\left(\frac{\sigma_y}{P}\right)\right\}\\ x_2 \geq \max\left\{\frac{\bar{N}_t}{P};\left(\xi\frac{l\tan\alpha}{2}\sqrt{\bar{N}_t/E}\right)\left(\frac{\sigma_y}{P}\right)\right\}\\ x_3 \geq \frac{\bar{T}}{P}\\ x_4 \geq \frac{T_t}{P}\\ x_5 \geq \max\left\{-\tilde{N}_{[1]}(\mathbf{x});1\right\}\\ x_6 \geq \max\left\{-\tilde{T}_{ct[1]}(\mathbf{x});0\right\}\\ x_7 \geq 0\\ \boldsymbol{K}\succeq\mathbf{0}\end{cases}. \tag{14}$$

In determining $\mathcal{X}$ we have considered that the unloaded state is the most severe for principal cables and tranversal struts, whereas the loaded state is the most severe for principal struts and tranversal cables. Finally, our

constrained minimum problem can be written as

$$\min\left\{\rho(\mathbf{x}) \;\middle|\; \mathbf{x}\in\mathcal{X}\right\}. \tag{15}$$

3. Numerical results

A slab of thickness $H = 100$ mm has been considered. The material has Young modulus $E = 200$ GPa and yield stress $\sigma_y = 200$ MPa. The struts have thin annular sections, with ratio between the average radius and the thickness equal to 10, corresponding to $\xi = \sqrt{\frac{2}{5\pi}}$.

The optimization problem has been solved for 30 different values of the uniaxial macro-stress Σ in the range $[10^{-5}, 10^{-1}]$ MPa. The local solver *fmincon* of *Matlab 2016* has been adopted and the *active-set* algorithm has been chosen. The algorithm requires an initial estimation $\mathbf{x}^{(0)}$ of the optimal solution, that in the present case has been set as

$$\mathbf{x}^{(0)} = \left\{ \begin{array}{l} x_1^{(0)} = 1.1\max\left\{\frac{N}{P}; \left(\xi\frac{l}{2}\sqrt{N/E}\right)\left(\frac{\sigma_y}{P}\right)\right\} \\ x_2^{(0)} = 1.1\max\left\{\frac{\bar{N}_t}{P}; \left(\xi\frac{l\tan\alpha}{2}\sqrt{\bar{N}_t/E}\right)\left(\frac{\sigma_y}{P}\right)\right\} \\ x_3^{(0)} = 1.1\dfrac{\bar{T}}{P} \\ x_4^{(0)} = 1.1\dfrac{T_t}{P} \\ x_5^{(0)} = 1.1\max\left\{-\tilde{N}_{[1]}(\mathbf{x}); 1\right\} \\ x_6^{(0)} = 1.1\max\left\{-\tilde{T}_{ct[1]}(\mathbf{x}); 0\right\} \\ x_7^{(0)} = 0.1 \end{array} \right\}. \tag{16}$$

Fig. 3 is the log-log graph of the volume density versus Σ for the three tensegrity shapes here considered. Interestingly we find a quasi-linear dependence for all shapes. As the figure shows, the exagonal shape is the most convenient.

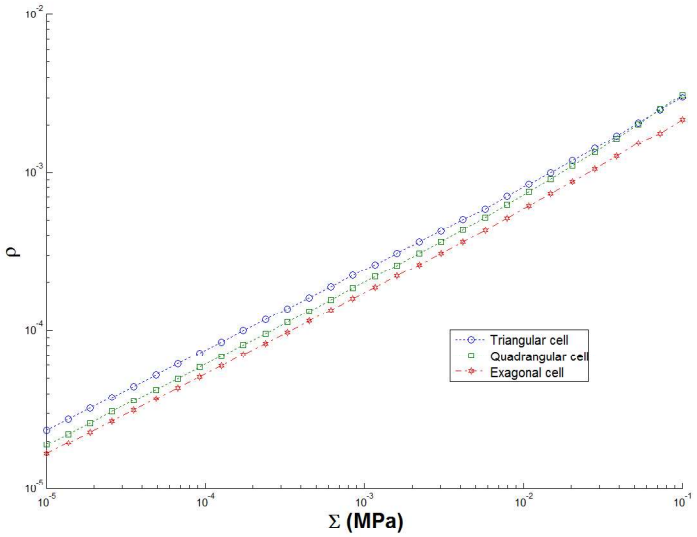


Figure 3: Optimal volume density

In Fig. 4 we represent the optimal value of the geometrical parameter $\tan\alpha$ for the three different shapes. Notice that the optimal values for the quadrangular and triangular shapes are almost equal. Moreover, in all cases the optimal $\tan\alpha$ changes slightly with respect to the macro-stress Σ, so determining an almost constant cell dimension. This is a remarkable result of our approach in the perspective of new materials design.

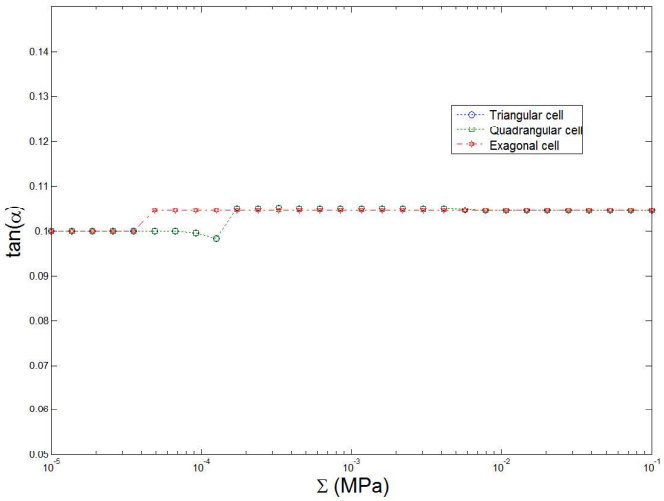


Figure 4: Optimal values of $\tan\alpha$

In Fig. 5 the optimal prestress parameter β for the three different shapes is represented. Notice that the optimal values of the quadrangolar and hexagonal shapes are almost coincident and varies slightly with respect to the macro-stress Σ, wheras the optimal values relative to the triangular shape exhibits a more complex behavior.

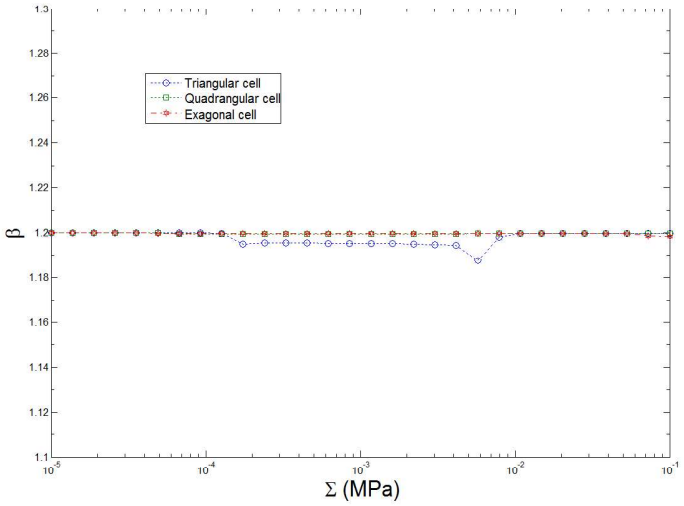


Figure 5: Optimal values of the prestress parameter β the prestress

Acknowledgments

This research was carried out in the framework of the ReLUIS-DPC 2016 project (Special Project RS11) funded by the Italian Department of Civil Protection.

[1] Motro R. Tensegrity. Kogan Page Science, London, 2003

[2] Zheng X et al. Ultra-light, Ultra-stiff Mechanical Metamaterials. Science 2014; 344: 1373–1377.

[3] Bückmann T, Stenger N, Kadic M, Kaschke J, Frölich A, Kennerknecht T, Eberl C, Thiel M, Wegener M. Tailored 3D Mechanical Metamaterials Made by Dip-in Direct-Laser-Writing Optical Lithography. Adv. Mater. 2012; 24: 2710–2714

[4] Chen H, Chan C. T., Sheng P. Transformation optics and metamaterials. Nature Materials 2010; 9: 387–396

[5] Fraternali F, Carpentieri G, Amendola A, Skelton RE, Nesterenko VF. Multiscale tunability of solitary wave dynamics in tensegrity metamaterials. Applied Physics Letters 2014; 105: 201903

[6] Paulose J, Meeussen AS, Vitelli V. Selective buckling via states of self-stress in topological metamaterials PNAS 2015; 112: 7639–7644

[7] Fang N, Xi D, Xu J, Ambati M, Srituravanich W, Sun C, Zhang X. Ultrasonic metamaterials with negative modulus. Nature materials 2006; 5: 452–456

[8] Schittny R, Bückmann T, Kadic M, Wegener M. Elastic measurements on macroscopic three-dimensional pentamode metamaterials. Applied Physics Letters 2013; 103:1905

[9] De Tommasi D, Marano GC, Puglisi G and Trentadue F. Optimal complexity and fractal limits of self-similar tensegrities. Proc. R. Soc. A 2015; 471: 20150250

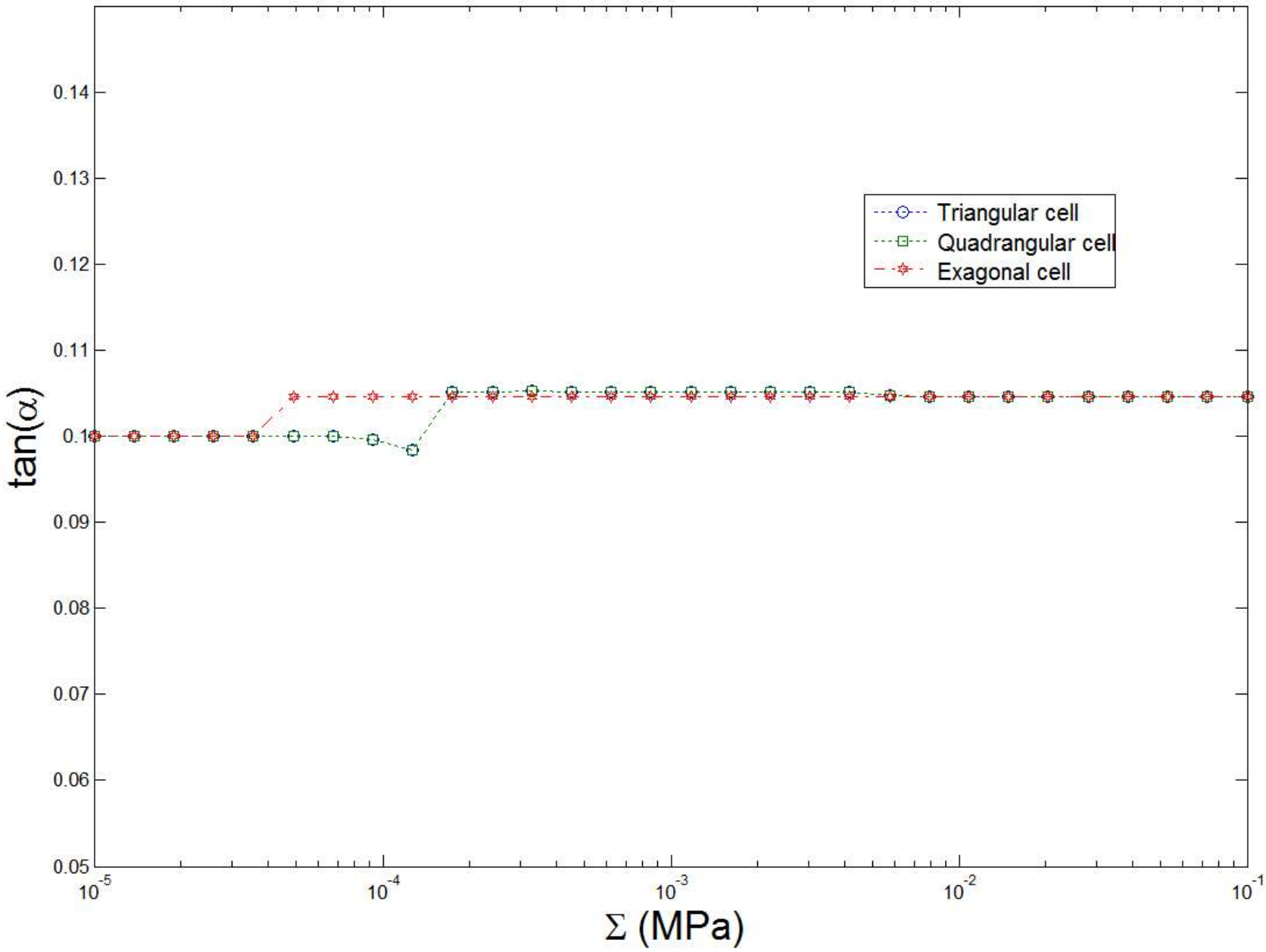
[10] De Tommasi D, Maddalena F, Puglisi G and Trentadue F, Self organized criticality and fractality of minimal mass structures, submitted (2016)

[11] Lee S, Gan BS, Lee J, A fully automatic group selection for form-finding process of truncated tetrahedral tensegrity structures via a double-loop genetic algorithm. J. Composite B 2016; 106: 308-315

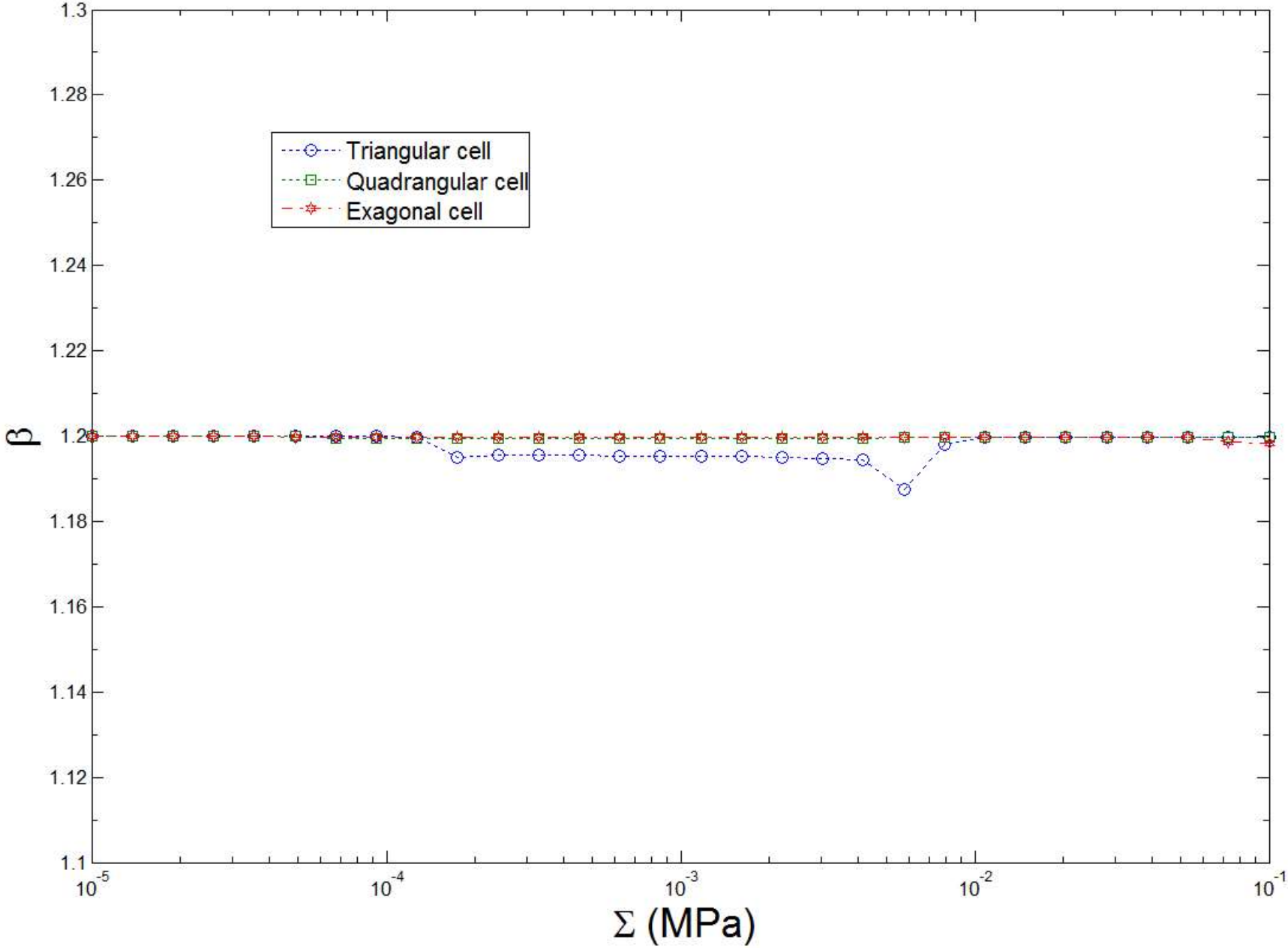
[12] Tibert AG, Pellegrino S, Review of Form-Finding Methods for Tensegrity Structures. Int. J. Space Struct; 18: 209-223

[13] Skelton RE, de Oliveira MC. Tensegrity systems 2009, Springer

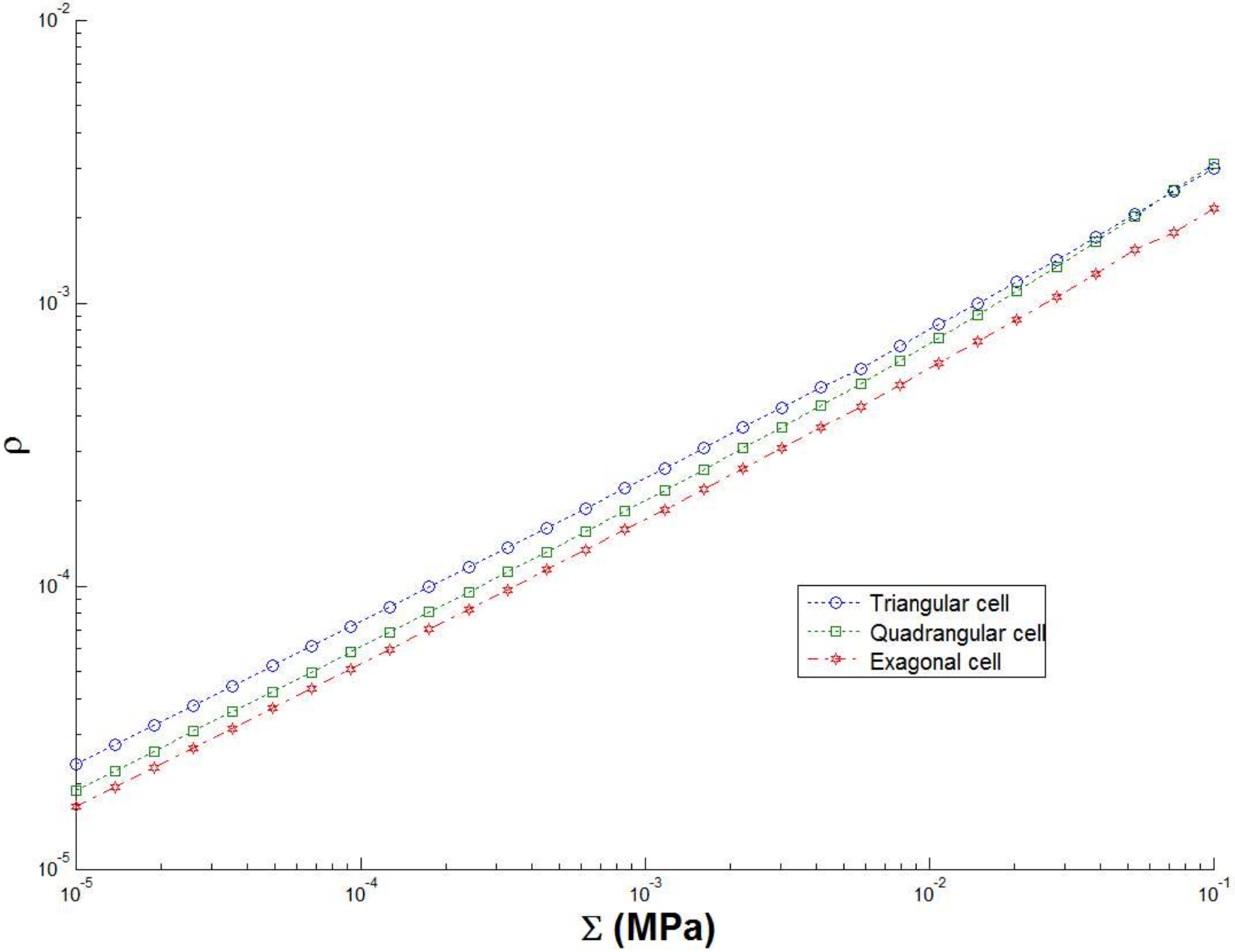
Figure


0.14
0.13
0.12
0.11
0.1
0.09
0.08
0.07
0.06
0.05
tan(α)
10^-5
10^-4
10^-3
10^-2
10^-1
Σ (MPa)
Triangular cell
Quadrangular cell
Exagonal cell

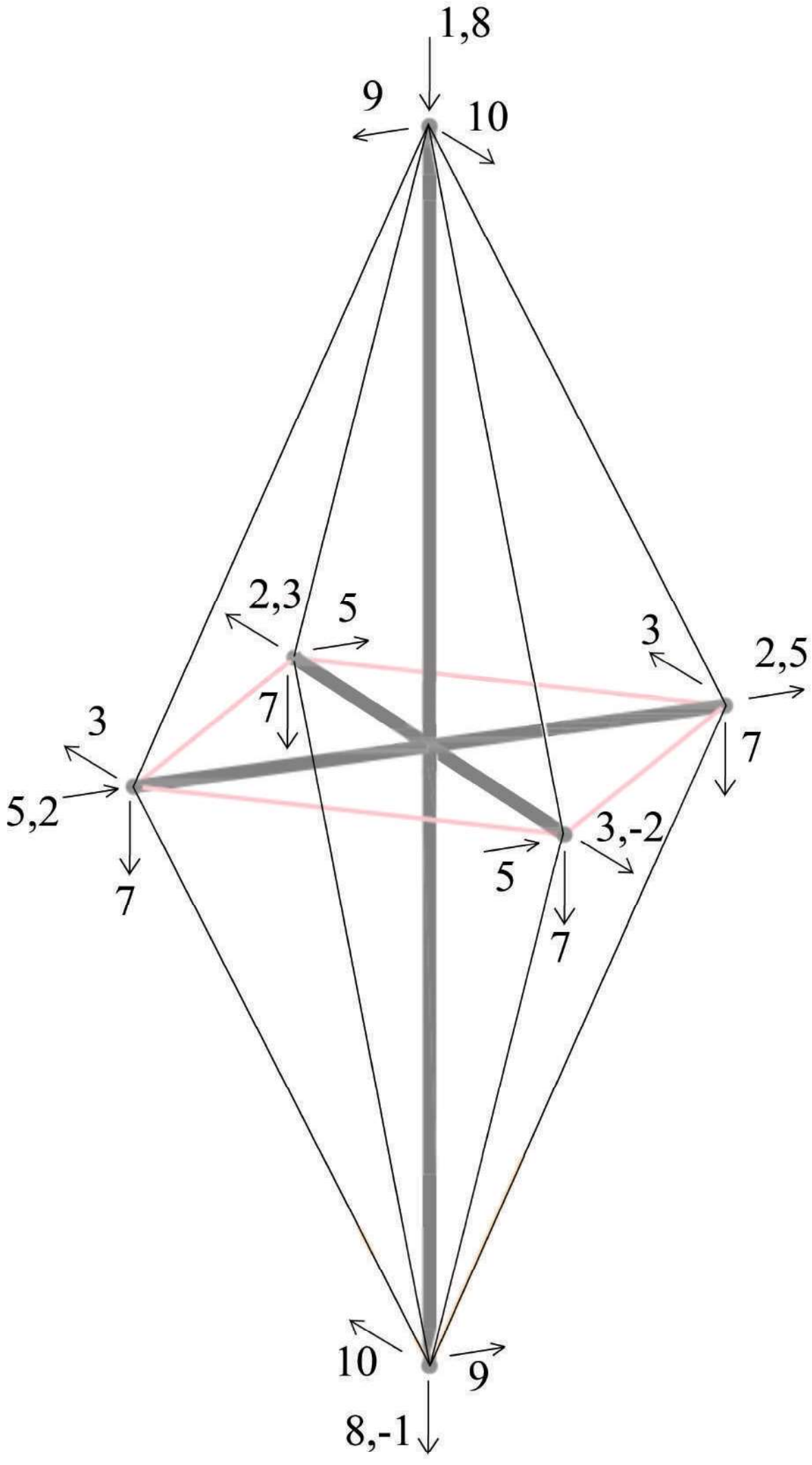
Figure


Triangular cell
Quadrangular cell
Exagonal cell
β
Σ (MPa)
1.3
1.28
1.26
1.24
1.22
1.2
1.18
1.16
1.14
1.12
1.1
10^-5
10^-4
10^-3
10^-2
10^-1

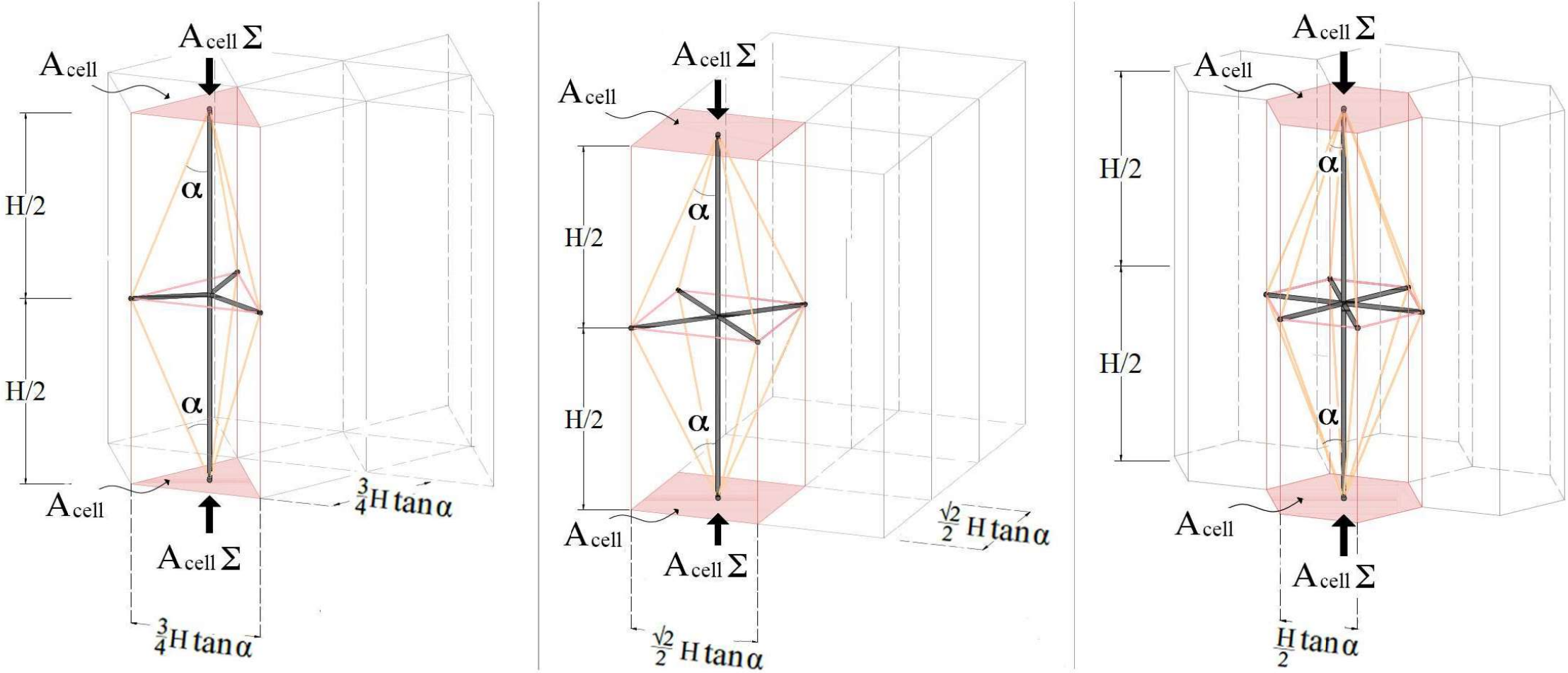
Figure


10^{-2}
10^{-3}
10^{-4}
10^{-5}
ρ
10^{-5}
10^{-4}
10^{-3}
10^{-2}
10^{-1}
Σ (MPa)
Triangular cell
Quadrangular cell
Exagonal cell

Figure



Figure


A cell Σ
A cell
α
H/2
H/2
α
A cell
A cell Σ
3/4 H tan α
3/4 H tan α
A cell Σ
A cell
α
H/2
H/2
α
A cell
A cell Σ
√2/2 H tan α
√2/2 H tan α
A cell Σ
A cell
α
H/2
H/2
α
A cell
A cell Σ
H/2 tan α

LaTeX Source Files

Click here to download LaTeX Source Files: Morphological1908.tex